Tuning optical properties of ZnO nanorods through doping with Au, Cu, Pt, Ni, and Gr nanoparticles

K. M. Ibrahim [a,*], W. R. Saleh [b], A. Y. Taradh [c]
[a] *Department of Physics, College of Education for Pure Science Ibn AL-Haitham, University of Baghdad, Baghdad, Iraq*
[b] *Department of Physics, College of Science, University of Baghdad, Baghdad, Iraq*
[c] *Laser Institute for Postgraduate Studies, University of Baghdad, Baghdad, Iraq*

This research focuses on the comparative analysis of the optical properties of zinc oxide (ZnO) nanorods doped with different nanoparticles (Au, Cu, Pt, Ni, and Gr). Both undoped and doped ZnO samples were prepared using a mixing procedure under identical conditions. X-ray diffraction pattern certain ZnO nanorods with hexagonal wurtzite structure and shown succeeded doping with (Au, Cu, Pt, Ni, and Gr) nanoparticles. Fourier Transform Infrared (FT IR), UV-visible, and photoluminescence (PL) spectroscopy were used to examine the modification in the optical properties of the samples due to the doping procedure. The results displayed considerable changes in the optical properties of ZnO nanorods after doping, including variations in emission peaks and energies of band gap, which refer to the institution of defects in structure and charge transfer processes. These results indicate that doped ZnO nanorods have scope applications in optoelectronics, biomedicine, and electronics.

(Received July 24, 2025; Accepted November 13, 2025)

Keywords: ZnO nanorods, Au, Cu, Pt, Ni, and Gr, Optical properties

1. Introduction

Nanotechnology represents a rapidly developing field within the interdisciplinary research environment of material sciences. Remarkable chemical and physical properties are due to the unique conformation and distribution of nanoparticles (NPs) with large surface area to volume ratios. Nanostructured metal oxide semiconductors (MOS) such as copper oxide, titanium dioxide, zinc oxide, calcium oxide, silver oxide, and magnesium oxide MgO have been studied [1]. Among these substances, the ZnO NPs are nanomaterials that have been widely used in different fields and applications due to their important properties, such as medicine, energy, environment, and communications. These properties, including microwave absorbing, good thermal stability, high electron mobility, large exciton binding energy, infrared shielding properties, photocatalytic properties, considerable energy bandgap, chemical stability, optical transparency, nontoxicity, availability, and cost-effectiveness [2,3]. Many factors, such as doping concentration, processing conditions, and method of doping, influenced the optical properties, structure, and morphology of doped ZnO and led to noticeable differences from the pure material [4]. ZnO doped with transition metals has been shown as a potential method of changing its electrical and optical properties. The ZnO doped with transition metal ions is a flexible way to develop execution for biomedicine, electronics, and optoelectronics [5]. The combination of metal ions such as Cr, Mg, Ce, Ga, Fe, Al, Mn, or Cu into ZnO through doping inserts structural defects, especially oxygen vacancies, which promote processes of charge transfer. This can be achieved by doping with (e.g., Co, Au, Ni, Pt) to develop hybrid nanostructures. Defect sites generated by these modifications that trap electrons, thereby improving the electron-hole pair separation and enhancing the electronic properties or photocatalytic. [3,6].

* Corresponding author: cajeen.m.i@ihcoedu.uobaghdad.edu.iq
https://doi.org/10.15251/JOR.2025.216.761

On the other hand, graphene, a p-type nanomaterial renowned for its exceptional electron mobility, chemical stability, and thermal conductivity, has featured as one of the most widely studied substances across diverse applications. Graphene-based semiconductor composite photocatalysts have garnered importance owing to their capability to use solar energy and change it into chemical energy. This capability positions graphene-based systems as a promising solution to focus global challenges related to the energy crisis and environmental degradation [7, 8]. The major goal of this study is to show a comparative study of the optical properties of ZnO nanoparticles (NPs) doped with various metal nanoparticles (Au, Cu, Pt, Ni) and graphene (Gr). These materials were chosen due to their capability to replace ions of ZnO lattice, enabling the creation of modified ZnO NPs with potential for new applications.

Both undoped and doped ZnO films were prepared using a mixing procedure under identical conditions. X-ray diffraction was used to analyze changes in the structural parameters of the nanostructured films resulting from the different doping processes. FT-IR, UV-visible, and PL spectroscopy were performed to study the alteration in the optical properties of ZnO nanostructures due to the doping process with different nanoparticles.

2. Experimental work

2.1. Chemical materials

To prepare ZnO nanorods, zinc acetate dihydrate (Zn $(CH_3COO)_2.2H_2O$), 98%, E. Merck Darmstadt Co., Germany) Moreover, (NaOH, 99%, Applichem Gmbh) were used. Au NPs with purity of >99.97% APS: 28nm, bulk density ~ 0.85 g/m^3, supplied by US Research Nanomaterials, Inc. Cu NPs, APS of 30 nm surface area 15 (m^2/g) purity of 99.9%, from Nanjing H T Nano Material Co., Ltd. Pt NPs purity of 99.9%, nano powder < 25 nm, Nanografi Co. Ni NPs, nano powder < 100 nm, 99.9% metals basis, from Aldrich. Gr with purity of >99.5+ %, 28 nm supplied by US Research Nanomaterials, Inc. Filtered water, Ethanol, and Methyl alcohol of 99.9% were used as rinsing and solvent agents through the prepared process.

2.2. Prepared doped ZnO nanorods

ZnO NRs were prepared in our previous research by the hydrothermal method [9]. The pure zinc oxide (ZnO) powder was first ground in a mortar for about two minutes. After grinding, it was dissolved in methanol and then applied to a cleaned glass substrate using the doctor blade coating. The glass substrate had been thoroughly cleaned beforehand by washing it multiple times with distilled water and Ethanol.

For the doped samples, nanoparticles of Au, Cu, Pt, Ni, and Gr were used, each making up a 3% percentage. From research in the laboratory and based on previous experiments, the percentage of doping was chosen. With 1 ml of methanol, each one of the nanoparticles was separately mixed and stirred by an ultrasonic for five min to create a uniform suspension. In the meantime, ZnO was also mixed with 1 ml of methyl alcohol to form a harmonious spreading through mixing. Finally, the suspensions of nanoparticles were individually inserted into the ZnO solution and 10 min mixed to obtain a homogeneous mixture.

2.3. Characterization techniques

By using different techniques, the samples were analyzed to understand their structure and optical properties. X-ray diffraction with a Lab XRD-6000 instrument was used to examine their crystal structure. This involves employing CuK-alpha radiation (wavelength of 1.54060 Å) and settings of 30 mA current and 40 kV voltage. The samples were scanned at angles ranging from 20° to 80°.

(FTIR) spectrometer was used to identify the chemical bonds and functional groups in the samples, and the measurements were taken with a maximum resolution of 0.5 cm^{-1}. Also, UV-vis spectrometer (OPTIMA SP-3000) with scanned wavelengths from 200 to 1100 nm was used. Additionally, the (PL) of the samples was investigated using an SL 174 spectrofluorometer, which

measured emission across a range of 300 to 900 nm. These analyses provided insights into the optical characteristics of the materials.

3. Results and discussion

3.1. XRD analysis

Fig. 1 displays the XRD patterns for the synthesized ZnO nanorods and for samples doped with Au, Cu, Pt, Ni, and Gr. The analysis is certain that the undoped ZnO nanorods have good crystallinity and confirm a hexagonal wurtzite structure (JPCDS number: 36-1451) [9]. It was clear from the distinguished diffraction peaks at 31.95°, 34.75°, 36.3°, 47.6°, 56.95°, 62.8°, and 68.65° equivalent to planes (100), (002), (101), (102), (110), (103), and (112), respectively. Also, the sharpness of peaks indicated that these nanorods are pure and without any impurities. When dopants are inserted into the crystal system, it leads to a shift of the main diffraction peaks to the low 2θ angles, and the intensities of these peaks are varied. Some weaker peaks of dopant crystalline nanomaterials (Au, Cu, Pt, Ni, and Gr), marked with "*," are attributed to the samples. Table 1 shows details of the XRD data of lattice cell parameters and crystallite size in the pure and doped ZnO nanorods. With doping, the lattice constants a and c varied, which verifies that the doping was successful. Pure ZnO displayed the smallest lattice constants (*a* and *c*) of 3.23004 and 5.153079 Å. With the insertion of impurities into the ZnO structure, there was a slight increase in the lattice constants. The Debye Scherrer formula used to calculate size of ZnO nanorods [10]:

$$D = \frac{0.89\,\lambda}{\beta\,cos\theta} \tag{1}$$

Where Scherer's factor is 0.89, λ is the X-ray's wavelength, 'θ' is the "Bragg diffraction angle," and 'β' is a invariable known as the "full width at half-maximum (FWHM)" of a deflection angle. The average size of particles of undoped ZnO nanorods related to the (FWHM) of the characteristic diffraction peaks at 31.95°, 34.75°, and 36.3° was found to be 11.1 nm. After doping with Au, Cu, Pt, Ni, and Gr, the average crystal size was 11.4, 12, 12.4, 11.2, and 11 nm, respectively.

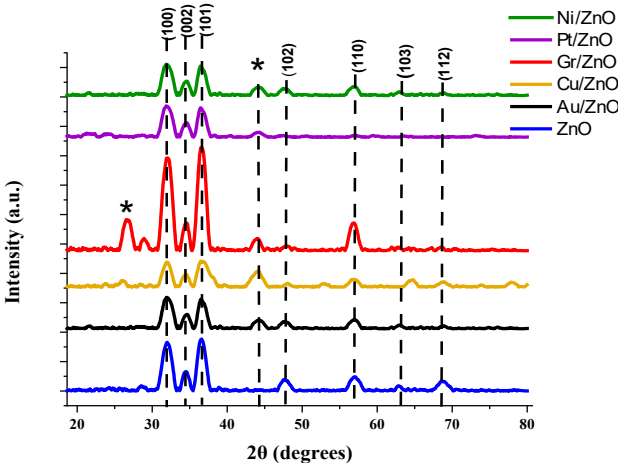

Fig. 1. XRD diffraction peaks of pure ZnO, doped ZnO with (Au, Cu, Pt, Ni, and Gr).

Table 1. Parameters obtained from XRD patterns of ZnO NRs doped ZnO with (Au, Cu, Pt, Ni, and Gr).

Sample	2θ (Deg.)	FWHM (Deg.)	d_{hkl} Exp.(Å)	C.S (nm)	hkl	*a* (Å)	*c* (Å)	D (nm)
ZnO	31.95	1	2.7973	8.3	(100)	3.230044	5.289725	11.1
	34.75	0.57	2.5874	14.6	(002)			
	36.3	0.8	2.4728	10.5	(101)			
Au/ZnO	31.9	1	2.8031	8.3	(100)	3.236794	5.2634	11.4
	34.52	0.61	2.5962	13.6	(002)			
	36.28	0.68	2.4741	12.3	(101)			
Cu/ZnO	31.8	0.8	2.8117	10.3	(100)	3.246709	5.165186	12
	34.5	0.61	2.5976	13.7	(002)			
	36.35	0.7	2.4695	11.9	(101)			
Gr/ZnO	31.91	0.74	2.79848	11.2	(100)	3.231406	5.218695	12.4
	34.55	0.61	2.5940	13.6	(002)			
	36.4	0.75	2.4663	11.2	(101)			
Pt/ZnO	31.92	0.9	2.8014	9.2	(100)	3.234819	5.262043	11.2
	34.6	0.67	2.5903	12.4	(002)			
	36.3	0.7	2.4728	11.9	(101)			
Ni/ZnO	31.91	0.9	2.8023	9.2	(100)	3.235806	5.194209	11
	34.58	0.65	2.5918	12.8	(002)			
	36.4	0.75	2.4663	11.2	(101)			

3.2. FT-IR

FTIR spectroscopy was used to examine the functional groups in the formation of pure and doped ZnO with Au, Cu, Pt, Ni, and Gr nanomaterials. The FTIR spectra of all samples shown in Figure 2 in the range of (400 – 4000) cm-1, different functional groups were shown and chemisorbed types in samples. At 568 cm-1, a peak appeared to indicate the presence of the stretching Zn–O vibration. The C–O vibration mode exists at peaks 1037 to 1102 cm-1. For pure ZnO, at 1469 cm^{-1} and 1500 cm^{-1} may indicate existence of C=O groups [11].

At different wavenumbers in the undoped ZnO spectrum, the stretching vibration of the functional group C-H was observed. Symmetric and asymmetric modes match peaks centered at 2909 cm^{-1} and 2920 cm^{-1}, respectively, in the band [12]. Modes of stretching vibration (O–H) of water molecules agree with the band around 3422 cm-1 [13].

The FTIR spectra of doped ZnO displayed some changes compared to undoped ZnO, because of the variance between the radii of the ionic dopants and Zn2+. This leads to the existence of a shift in the spectra and assists in the substitution of Zn2+ by ions of dopants. It confirms the combination of dopants in the lattice of ZnO.

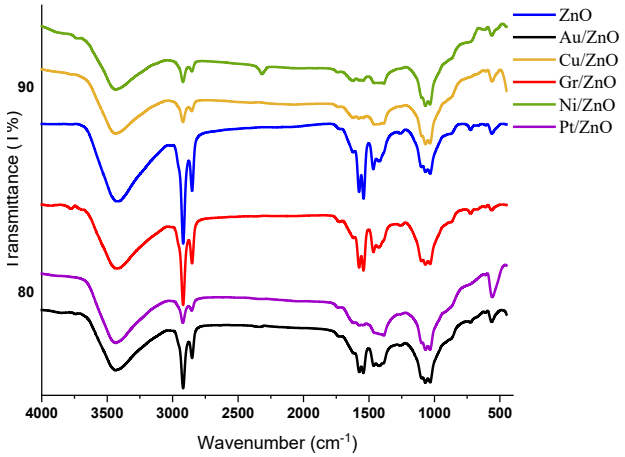

Fig. 2. FTIR of pure ZnO, Au, Cu, Pt, Ni, and Gr doped ZnO

3.3. UV–visible

Figure (3a) presents the spectra of UV–visible absorption of ZnO undoped and doped with Au, Cu, Pt, Ni, and Gr nanostructures. The properties of undoped ZnO and doped ZnO nanorods were effectively studied. The band gap of these nanostructures changes as the various nanoparticle dopants can produce various crystal defects in the structure of the ZnO. The absorption peak is strong at the wavelength (300) nm as the spectrum indicated, because the absorption of the bandgap for zinc oxide results from electrons removed from the valence-band to the conduction-band. Zinc oxide nanorods have good absorption in the UV region and a sharp peak of absorption appears because ZnO particles are nano-sized down to ~11 nm and the particle size distribution is narrow [1]. Compared to pure ZnO, the UV spectra shapes for doped–ZnO significantly change; this is referred to as the synergistic interaction of the (Au, Cu, Pt, Ni, and Gr) nanostructures dopants with ZnO [2]

In the UV region, the absorbed level of ZnO is relatively substantial within the wavelength domain of (300-400) nm and begins the absorption to decrease at wavelengths above 350 nm. For the doped ZnO, the absorption, in general, is higher. Simultaneously, the energy gap of the doped ZnO is decreasing. The Au, Cu, Pt, Ni, and Gr nanostructure dopants had considerable influence on the optical properties of the ZnO nanorods. They made new energy states in the band gap by modifying the electronic band structure, hence changing the optical properties of ZnO nanorods. Tauc relationship was used to estimate the optical bandgap energies of samples as in Eq.2 [3]:

$$(\alpha h\upsilon) = B\ (h\upsilon - Eg)^r \tag{2}$$

where α refers to the coefficient of absorption; h is the Planck constant; $h\upsilon$ is the energy of incident photon; a constant B is known as the Tauc parameter, which has crucial information about the structure of the material; E_g stands for the energy band gap; and r denotes a particular coefficient which depends on the electronic transition type; it can take two values depending on the transition whether direct transition ($r = \frac{1}{2}$) or indirect transition ($r = 2$). From Fig. 3 b, the optical transition is direct, and the band gap E_g of ZnO is 4 eV. This high value of Eg indicates that a wide bandgap of valuable material characterizes the ZnO nanorods in many optoelectronic applications [4]. The doped ZnO samples with Au, Cu, Pt, Ni, and Gr nanostructures have E_g of 3.9 eV for Cu/ZnO and Gr/ZnO, 3.7 eV for Au/ZnO, Pt/ZnO, and Ni/ZnO, respectively. It remarked that the values of the E_g of the doped ZnO nanorods decreased in contrastto pure ZnO. The responsible for causing the decrease of bandgaps after doping is the existence of oxygen vacancies that assist the easy transmission of electrons from V.B. to C.B [3].

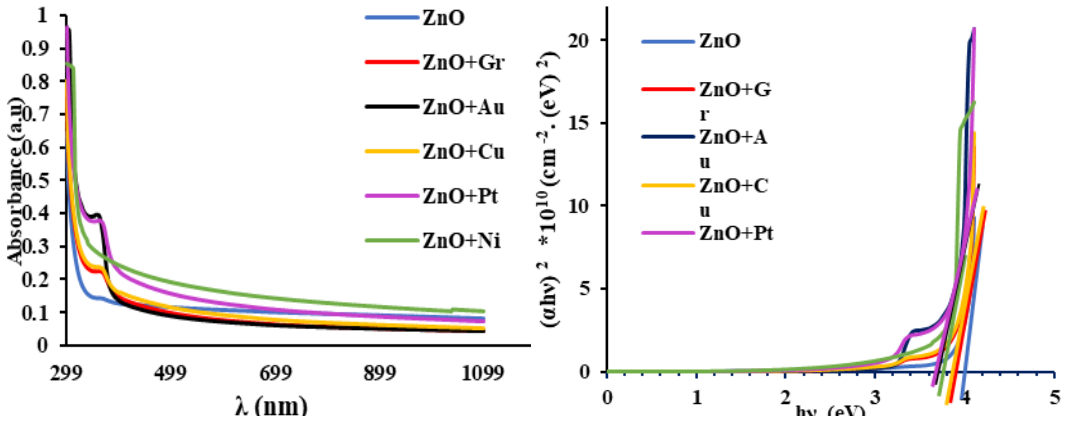

Fig. 3. a) UV–visible absorption spectra, b) Optical bandgaps of undoped ZnO, Au, Cu, Pt, Ni, and Gr doped ZnO.

3.4. PL analysis

PL spectra are signals in which the recombination of carriers photogenerated can be characterized where the lifetime of electron-hole pairs is closely related to photocatalytic activity. At room temperature, the PL of the ZnO nanorods and the doped ZnO with Au, Cu, Pt, Ni, and Gr nanostructures with an excitation wavelength of 300 nm are shown in Figure (4). The PL spectra show a clear excitonic UV emission and a broad peak spanning the UV long-wave range to blue. In the UV region the emission peaks centered at nearly 299 nm (4.14 eV) for pure ZnO, 300.93 nm (4.12 eV) for Au, Pt, and Ni-doped ZnO, 310 nm (4 eV) for Cu/ZnO, and 307 nm (4.02 eV) for Gr/ZnO, identical to the near band-edge emission (NBE) product from the recombination of the free exciton. The energy band gap was determined by means of the PL spectra from the Eq.3 [17]:

$$E_g=1240/\lambda \tag{3}$$

In the meantime, the broad emission peaks, in general, are due to the recombination procedure of the intrinsic defects of ZnO inside the band gap at different levels; these are generally called deep-level emissions (DLE) [16].

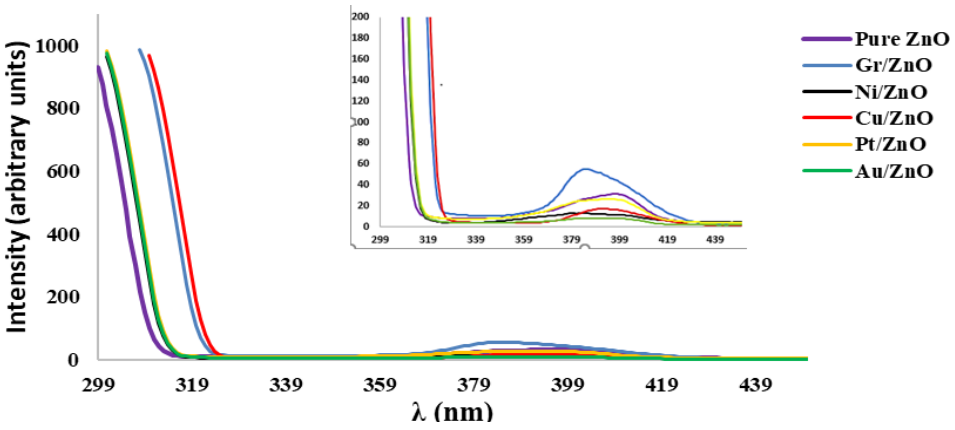

Fig. 4. PL spectra of Pure ZnO Au, Cu, Pt, Ni, and Gr doped ZnO.

4. Conclusions

In this work, ZnO nanorods and ZnO doped with (Au, Cu, Pt, Ni, and Gr) were prepared and investigated. XRD is certain the hexagonal wurtzite structure of ZnO. Sharp peaks indicated good crystallinity, slight shifts in diffraction peaks to lower 2θ angles, variations in intensities confirmed dopant insertion and weak peaks of dopant crystalline nanostructures appeared. FTIR confirmed the presence of various functional groups and chemisorbed species, where the Zn-O Vibration Peak was 568 cm^{-1}. Changes in FTIR spectra due to differences in ionic radii between dopants and Zn^{2+} confirm dopant incorporation.

The spectrum of UV- vis of pure ZnO displays a strong peak of absorption at 300 nm because of nanosized particles. Doped ZnO showed significant changes in UV spectra and increased absorption in the 300-400nm range. The Tauc relationship is used to calculate the band gap. The energy band gap of undoped ZnO was 4 eV, while doped ZnO decreased by 3.9 eV for Cu/ZnO and Gr/ZnO, 3.7 eV for Au/ZnO, Pt/ZnO, and Ni/ZnO, respectively. PL showed the Excitonic UV Emission was at 299 nm (4.14 eV) for pure ZnO, 300.93 nm (4.12 eV) for Au, Pt, and Ni-doped ZnO, 310 nm (4 eV) for Cu/ZnO, and 307 nm (4.02 eV) for Gr/ZnO, corresponding to the near band edge. Meantime, the broad emission peaks in general due to the recombination procedure of the intrinsic defects of ZnO inside the band gap in different levels; these are generally called deep level emissions DLE.

The decrease in band gap with doping makes these materials potentially useful for various optoelectronic and photocatalytic applications.

References

[1] S. Vikalm, S. Vikal, Y. K. Gautam, A. K. Ambedkar, D. Gautam, J. Singh, D. Pratap, A. Kumar, S. Kumar, M. Gupta, B. P. Singh, Jou. of Sem., 43 (3), p. 032802, (2022); https://doi.org/10.1088/1674-4926/43/3/032802

[2] Z. M. AL-Asady, A. H. AL-Hamdani, M. A. Hussein, in AIP conference proceedings, AIP Publishing, 2213 (1), (2020).

[3] L. Arda, Z. Raad, S. Veziroglu, C. Tav, U. Yahsi, J Mol Struct, (1320), p. 139663, (2025); https://doi.org/10.1016/j.molstruc.2024.139663

[4] A. T. Naziba, M. T. Nafisa, R. Sultana, M. d. F. Ehsan, A. R. M. Tareq, R. Rashid, H. Das, A.K.M. A. Ullah, A.K.M. F. Kibria, J Magn Magn Mater, (593), p. 171836, (2024); https://doi.org/10.1016/j.jmmm.2024.171836

[5] M. H. Rashid, S. I. Sujoy, M. S. Rahman, M. J. Haque, Heliyon, 10 (3), (2024); https://doi.org/10.1016/j.heliyon.2024.e25438

[6] A. Mezni, N. B. Saber, M. M. Ibrahim, A. A. Shaltout, G. A. M. Mersal, N. Y. Mostafa, S. Alharthi, R. Boukherroub, T. Altalhi., J Inorg Organomet Polym Mater, (30), 4627-4636, (2020); https://doi.org/10.1007/s10904-020-01588-5

[7] M.-Q. Yang, Y.-J. Xu, The Journal of Physical Chemistry C, 117 (42), 21724-21734, (2013); https://doi.org/10.1021/jp408400c

[8] Z. Rafiee, H. Roshan, M. H. Sheikhi, Ceram Int, 47 (4), 5311-5317, (2021); https://doi.org/10.1016/j.ceramint.2020.10.111

[9] K. M. Ibrahim, W. R. Saleh, in AIP Conference Proceedings, AIP Publishing, 2922 (1), (2024).

[10] T. Seydioglu, S. Kurnaz, E. A. Tokeşer, G. Yildirim, O. Ozturk, Microsc Res Tech, 87(11), 2687-2700, (2024); https://doi.org/10.1002/jemt.24635

[11] I. Ngom, N. M. Ndiaye, A. Fall, M. Bakayoko, B. D. Ngom, M. Maaza, MRS Adv, 5 (21-22), 1145-1155, (2020); https://doi.org/10.1557/adv.2020.212

[12] S. B. Rana, R. P. P. Singh, Jou. of Mat. Sci.: Materials in Electronics, (27), 9346-9355, (2016); https://doi.org/10.1007/s10854-016-4975-6

[13] I. Ben Elkamel, N. Hamdaoui, A. Mezni, R. Ajjel, L. Beji, RSC Adv, 8 (56), 32333-32343, (2018); https://doi.org/10.1039/C8RA05567J

[14] E. G. Goh, X. Xu, P. G. McCormick, Scr Mater, (78), 49-52, (2014); https://doi.org/10.1016/j.scriptamat.2014.01.033

[15] S. H. Zyoud, V. Ganesh, C. A. C. Abdullah, I. S. Yahia, A. H. Zyoud, A. F. I. Abdelkader, M. G. Daher, M. Nasor, M Shahwan, H. Y. Zahran, M. S. A. El-sadek, E. A. Kamoun, S. M. Altarifi, M. Sh. Abdel-wahab, Crystals (Basel), 13 (7), p. 1087, (2023); https://doi.org/10.3390/cryst13071087

[16] K. M. Ibrahim, W. R. Saleh, A. M. A. Al-Sammarraie, Nano Hyb. and Com., (35), 75-83, (2022); https://doi.org/10.4028/p-0w806z

[17] W. R. Saleh, A. Y. Taradh, S. M. Hassan, F. T. Ibrahim, Jou. of Nano Res., (87), 21-31, (2025); https://doi.org/10.4028/p-Mym1uj